11th World Congress on Computational Mechanics (WCCM XI)
5th European Conference on Computational Mechanics (ECCM V)
6th European Conference on Computational Fluid Dynamics (ECFD VI)
E. Oñate, J. Oliver and A. Huerta (Eds)

A STUDY ON THE INFLUENCE OF DIRECTIONALITY ON BLAST-INDUCED BRAIN INJURY

HESAM SARVGHAD-MOGHADDAM[*], ASGHAR REZAEI[*], MEHDI SLAIMI- JAZI[*], GHODRAT KARAMI[*] AND MARIUSZ ZIEJEWSKI[*]

[*] Mechanical Engineering Department
North Dakota State University
111 Dolve Hall, Fargo, ND, 58108, USA
E-mail: g.karami@ndsu.edu, www.ndsu.edu

Key Words: *Brain Injury, Blast Wave, Directionality, ACH Helmet, Face Shield, Finite Elements.*

Abstract. Blast-induced traumatic injury (bTBI), a signature outcome of blast wave-head interaction is influenced by several parameters such as the blast intensity, the protection level of the head as well as the direction of the shockwaves with respect to the head. In this study, Finite Element (FE) simulation of the blast waves approaching from different directions with unprotected, helmeted, and helmet-face shield protected (fully-protected) heads is carried out. To comply with the lung injury threshold, an overpressure of 520 kPa is applied around the head. The main objective is to delineate the effect of blast directionality as well as different protection levels on the mechanical response of the brain. Propagation of the blast shockwaves and their interaction with the FE head model is simulated using a coupled multi-material Arbitrary Lagrangian Eulerian (ALE) technique along with the penalty-based algorithms. Head-shockwave interaction mechanism is investigated for the blast scenarios from the front, back, and side. All simulations are performed using LS-DYNA, a nonlinear finite element code used for high-speed impact modelling. The blast from the side is recognized as the worst scenario inducing the highest risk of injury in terms of the biomechanical parameters of the brain.

1 INTRODUCTION

Traumatic Brain Injury (TBI), known as the disruption of brain functionality due to a direct impact or the sudden movement of the head, is a signature outcome of blast shockwaves interaction with the head. The increasing incidence rate of blast-induced TBI (bTBI) has brought up the concern about the servicemembers safety in the battlefields mainly due to serious lifelong consequences of bTBI. It has been reported that out of 1.6 million personnel deployed in the Iraq war, around 160,000 members have been recognized to be suffering from mild bTBI [1]. In a clinical report, it has been estimated that more than 50% of blast-induced injuries lead to bTBI [2]. Unlike impact-induced TBI mechanism which mainly involves the acceleration and deceleration of the head, bTBI induces stress wave distribution inside the cranial medium.

Unlike numerous studies on the impact-induced TBI among the regular civilians and

servicemembers, fewer studies have addressed the issue of bTBI due to the complexity of the blast mechanism and the human head response upon exposure to blast shockwaves. Upon interacting with the head, any assault on the head in the form of high pressure gradient blast waves can introduce diffuse axonal injury, subdural haemorrhaging, and contusions [3]. Due to the moral issues of exposing human cadavers to blast waves, numerical methods such as finite element (FE) simulations have found a great application in assessing the response of human head under blast loading. Chafi *et al.* [4] carried out a comprehensive FE study on the biomechanics of the head when it is exposed to blast loading with different intensities. They mainly introduced the tissue-level responses of the brain, e.g. shear stress, shear strain and intracranial pressure (ICP) as the main injury predictors for the bTBI. They also found a direct correlation among these parameters. Ganpule *et al.* [5] investigated the blast flow dynamics around the head as well as the brain biomechanics due to interaction of head with frontal shockwaves using both experimental and numerical approaches. They determined the head geometry as the governing factor in blast flow dynamics and introduced the skull flexure and cavitation phenomena as the possible outcomes of bTBI. Rezaei *et al* [6] examined the influence of the environment confinement on the mechanical response of the head when exposed to indirect and direct blast waves. They observed higher ICP and shear stress values inside the brain for the confined space blast scenario. The role of body armour, especially the protective headgears in prevention of bTBI and increasing the survivability of the soldiers has been the subject of few studies. Moss *et al.* [7] observed high and low localized pressure gradients due to the skull flexure mechanism imposed upon the interaction of head with blast waves. They also introduced the underwash effect as the adverse effect of helmets which happens in the form of an amplified pressure region in the head-helmet gap and can be impeded by using the padding system. Grujicic *et al.* [8] studied the stress wave propagation within the brain for an unprotected and a helmeted head. Based on the blast loading conditions, they observed variable protection efficacy of the Advanced Combat Helmets (ACH). They reported complex temporal and spatial ICP and stress wave distribution in the intracranial space.

A brief look on the current literature shows that the geometry of the head as well as the implication of protective headgears may bring up unpredicted complications that can affect the biomechanics of the head. Different parameters such as the blast orientation and intensity, headgears shape as well as the head structural inhomogeneity may add up to this complications. So far, the role of blast wave orientation on the mechanical response of the unprotected and protected head as well as the likelihood of the bTBI have not been investigated. Accordingly, fluid-solid interaction of the blast waves approaching from the front, back and side directions with the unprotected, helmeted, and fully protected head (helmet and face shield together) is carried out. Using the FE model of the human head, ACH helmet, and the ballistic face shield, a blast overpressure of 520 kPa complying with the lung injury threshold proposed by Bowen *et al.* [9] is generated around the head for all loading conditions. The result will delineate the effect of blast wave directionality on the head response as well as the effectiveness of protective headgears in each blast scenario.

2 COMPUTATIONAL METHODS

2.1 FE discretization

A detailed model of the human head including the major components of the real head is used

for this study. This model was originally developed by Horgan and Gilchrist [10] from Magnetic Resonance Topography (MRT) images and was later completed by Chafi *et al.* [4] by inclusion of the neck muscle and bone as well as the facial bone and skin. This head model has been accurately validated against the experimental results of Nahum *et al.* [11] for a frontal impact on a cadaver head. Furthermore, geometries of the ACH helmet and the face shield were constructed via 3D image scanning and Solidworks software, respectively. The FE discretization of the head and protective headgears, shown in Figure 1(a-c), was mainly carried out using MSC/Patran [12] and Altair HyperMesh [13] software using 4-node shell elements and 8-node brick elements. Moreover, the helmet foam pads embedded in the 2.5 cm head-helmet subspace are modeled and meshed using HyperMesh. The aforementioned FE models form the Lagrangian section of our analysis. However, a $50 \times 50 \times 50$ cm cubic domain, shown in Figure 1(d), is constructed and meshed using HyperMesh to account for the Eulerian domain in which air and blast waves are modeled.

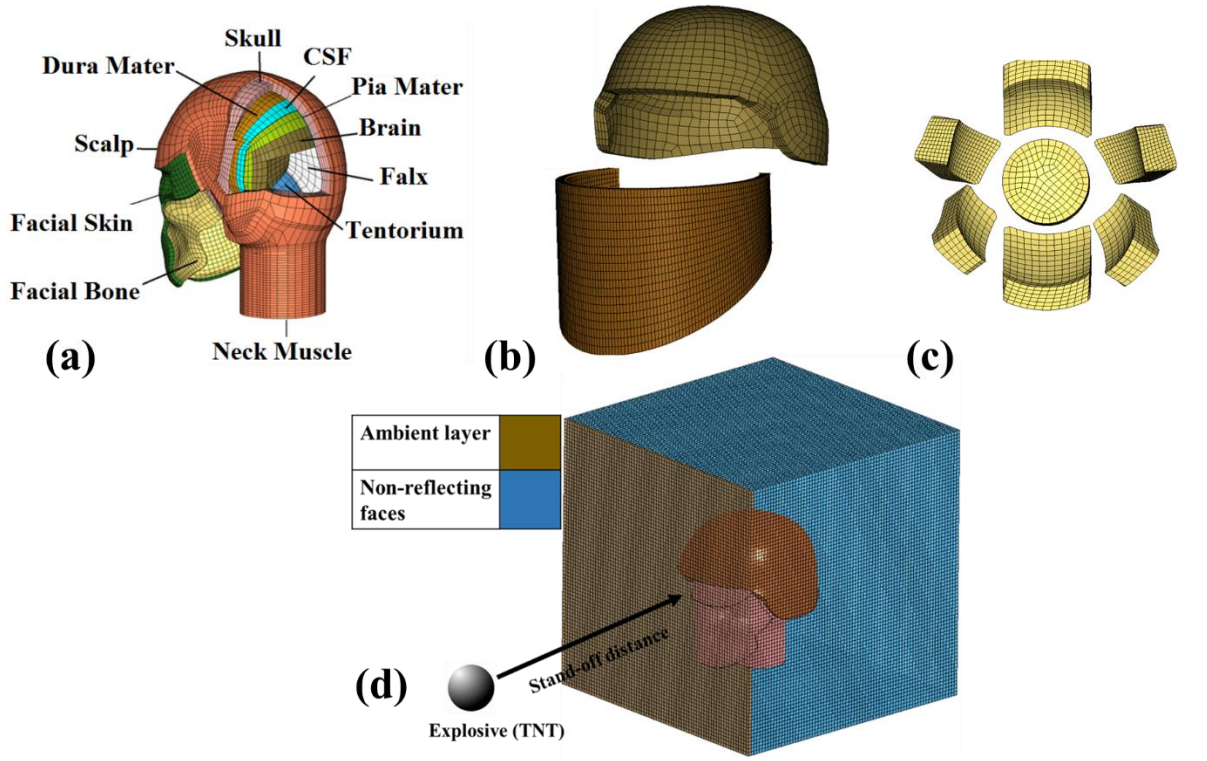

Figure 1: FE descritization of (a) head; (b) ACH helmet and face shield; (c) Padding system; and (d) ALE media

2.2 Material models

As the medium for the open blast scenario, air is modeled as an ideal gas at the ambient conditions using its equation of state: $p = (\gamma - 1)\frac{\rho}{\rho_0}E$ where p is the pressure, $\gamma = \frac{C_p}{C_v} = 1.4$ is the specific heat ratio for air, ρ and ρ_0 are the current and initial air density, respectively and E is the volumetric energy density.

Due to the significance of brain tissue response in TBI related studies, the most important material modeling pertains to this tissue. Several constitutive models have been considered for

this tissue, from linear elastic models to viscoelastic and hyper-viscoelastic models [11, 14 and 15]. However, brain undergoes large deformations when dynamic loads such as blast are applied to the head. Hence, in this study a hyper-viscoelastic constitutive law is employed to model the mechanical behavior of the brain tissue to accurately capture the nonlinear, viscous, and incompressible behavior of the this tissue. The brain material model adopted from the work of Mendis *et al.* [14] is presented in Table 1.

Table 1: Mechanical properties of hyper-viscoelastic brain material

C_{10}(Pa)	C_{01}(Pa)	G_1(kPa)	G_2(kPa)	$\beta_1(s^{-1})$	$\beta_2(s^{-1})$	K (GPa)
3102.5	3447.2	40.744	23.285	125	6.6667	2.19

However, in accordance with most of the literature on the impact and blast induced TBI, linear elastic material properties are chosen for the other head components and are presented in Table 2 based on the data provided by Willinger and Baumgartner [16] and Horgan and Gilchrist [10].

Table 2: Mechanical properties of the elastic head components

Component/ Tissue	**Mechanical Properties**		
	Density (kg/m^3)	Elastic Modulus (MPa)	Poisson's ratio
Scalp	1200	16.7	0.42
Skull	1800	15000	0.21
Dura, falx, tentorium	1130	31.5	0.45
Pia mater	1130	11.5	0.45
Neck bone	1300	1000	0.45
Neck muscle	1130	0.1	0.24
CSF	1040	Incompressible K=2.19 GPa	-

The transversely isotropic linear-elastic constitutive law is employed for modeling the Kevlar ACH helmet and the ballistic face shield. This model is adopted from the work of Van hoof *et al*. [17] and the material properties are presented in Table 3.

Table 3: Mechanical properties of the ACH helmet and the face shield

E_{11}=E_{22}**(GPa)**	E_{33} **(GPa)**	ν_{12}	$\nu_{23} = \nu_{31}$	G_{12} **(GPa)**	G_{13}= G_{23} **(GPa)**	$\rho(g/cm^3)$
18.5	6.0	0.25	0.33	0.77	2.715	1.23

E: Young's modulus, ν: Poisson's ratio; *G* shear modulus, **ρ**: Density.

Based on the analysis performed by Salimi Jazi *et al.* [18], the expanded polypropylene with a density of $31 kg/m^3$ is chosen for the foam pad material. The mechanical behavior of the foam material is adopted from the work of Kleiven and von Holst [19] and is shown in Table 4.

Table 4: Mechanical properties of the foam pad material

Type of the Foam	Density (Kg/m^3)	Yield Strength (kPa)	Plateau Strength (kPa)	Tangential Modulus (MPa)
Expanded Polypropylene (EPP)	31	100	100-250	1.9

2.3 Blast simulation

Load_Blast_Enhanced (LBE) approach and Multi-Material Arbitrary Eulerian-Lagrangian (MM-ALE) formulation are the two main numerical techniques in Ls-Dyna that have been used for modeling the blast. However, low accuracy as well as the inability of LBE method to model the shockwave reflections at the corners and the huge computational cost of MM-ALE method have led to the advent of the coupled method. This recent feature of Ls-Dyna inherits the advantages of LBE and MM-ALE techniques in order to provide an accurate simulation of blast waves with a reasonable computational cost. This is achieved through skipping the discretization of the domain between the explosive and the Lagrangian domain. In this method only an immediate air domain around the object of interest is modeled and the blast pressure from the detonation is calculated using empirical laws and is applied on the surface of the domain facing the explosive (ambient layer). An overpressure of 520 kPa around the head is generated through detonation of 70 grams of TNT placed 58 cm distant from the head (stand-off distance). As shown in Figure 2(b), the generated shockwaves by this method accurately models the essential characteristics of a Friedlander shockwaves (Figure 2(a)) such as, arrival time, overpressure duration, as well as the positive and negative pulse durations [20].

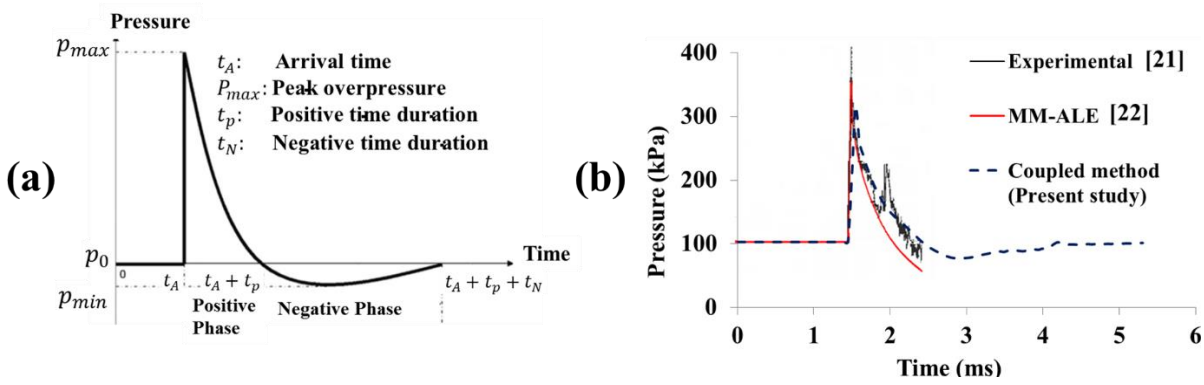

Figure 2 : (a) Friedlander Shockwave [20]; (b) Validation of coupled method against experiment and MM-ALE

2.4 Problem formulation and solution scheme

The interaction of blast-induced shockwaves approaching from front, back, and side with different assemblies of the head and protective headgears is carried out. Three levels of protection is considered: the unprotected head, head protected by padded ACH helmet (helmeted) and the head protected by the padded helmet and the face shield (fully-protected). In each scenario, a 520 kPa overpressure, representative of the lung injury threshold obtained from the curve of Bowen *et al.* [9] is considered. The blast flow dynamics, as well as the

response of brain under the blast loading is desired. The nonlinear transient FE solver, Ls-dyna, is employed for performing all simulations. The computational algorithm is mainly implemented through ALE formulation: first the solid deforms through the Lagrangian formulation and then the state variables of the deformed Lagrangian elements are mapped back onto the ALE reference mesh through an advection step. Finally, the governing conservation laws (mass, momentum, and energy) along with solid material constitutive relationships are solved simultaneously for the state variables. The fluid-structure interaction (FSI) between the Lagrangian domain (head and protective equipment) and the Eulerian domain (ALE media including air and propagating blast waves) is implemented through penalty based methods. The numerical approach is performed using the Operator Split method [23]. The procedure can be simply summarized as follows: the intersection of ALE and Lagrangian parts are found, the coupling points are recognized, the displacement of ALE fluid through Lagrangian segments is marked as the penetration distance and the loading evaluated based on this distance is distributed again on both ALE and Lagrangian materials [23]. All surfaces of the media except for the ambient surface facing the detonation, are modeled as non-reflecting boundaries to allow for the outflow of the propagating shockwaves in an open space blast scenario, as shown in figure 1(d). To achieve a more stable solution as well as preventing rigid body motion, the inferior surface of the neck is constrained in all degrees of freedom.

3 RESULTS AND DISSCUSION

In this study, the brain acceleration, ICP, and shear stress refer to the resultant center mass linear acceleration of the brain, the intracranial pressure, and the maximum shear stress, respectively and their quantities are calculated as an average of their values in a selected region. The temporal variation of shear stress and ICP are presented at the brain stem and coup site, respectively where the maximums occur. The duration of all simulations is 10 milliseconds, but only the first 5 milliseconds are plotted as no remarkable change occurs after this time.

3.1 Front blast scenario

The response of the unprotected, helmeted, and fully-protected heads under front blast loading is shown in figure 3. Significant reduction in ICP (77%) and brain acceleration (80%) is observed upon using the fully-protected assembly, while the helmeted case reduces the ICP and brain acceleration by 37% and 65%, respectively. Although, a major part of the dynamic load induced by the pressure waves traveling inside the head-helmet gap is disrupted by the pads in the helmeted case, the face shield further prevents the incoming waves from entering the gap leading to an extra attenuation of the pressure waves. The diffraction of the shockwaves by the face shield impedes their direct interaction with the face and head as the main pathways for blast wave propagation inside the cranial space, hence leading to an increased protection efficiency for the fully-protected system. Temporal variation of the local shear stresses inside the brain developed due to the hyper-viscoelastic nature of the brain tissue is shown in figure 3(b). The shear deformations can lead to diffuse axonal injuries which serve as the most devastating type of TBI and hence can disturb the functionality of brain. Although the fully-protected system damps the shear stresses by 15% due to the high protection against blast waves, the helmeted assembly doesn't make any change. As stated before, both helmeted and fully-protected systems provide significant attenuation of the acceleration. The reason lies

within the fact that while elevated inertial forces are experienced by the head due to the added mass by the protective headgears, the increase in the surface area affected by the shockwaves counteracts these forces and results in a remarkable attenuation of the acceleration, as seen in figure 3(c).

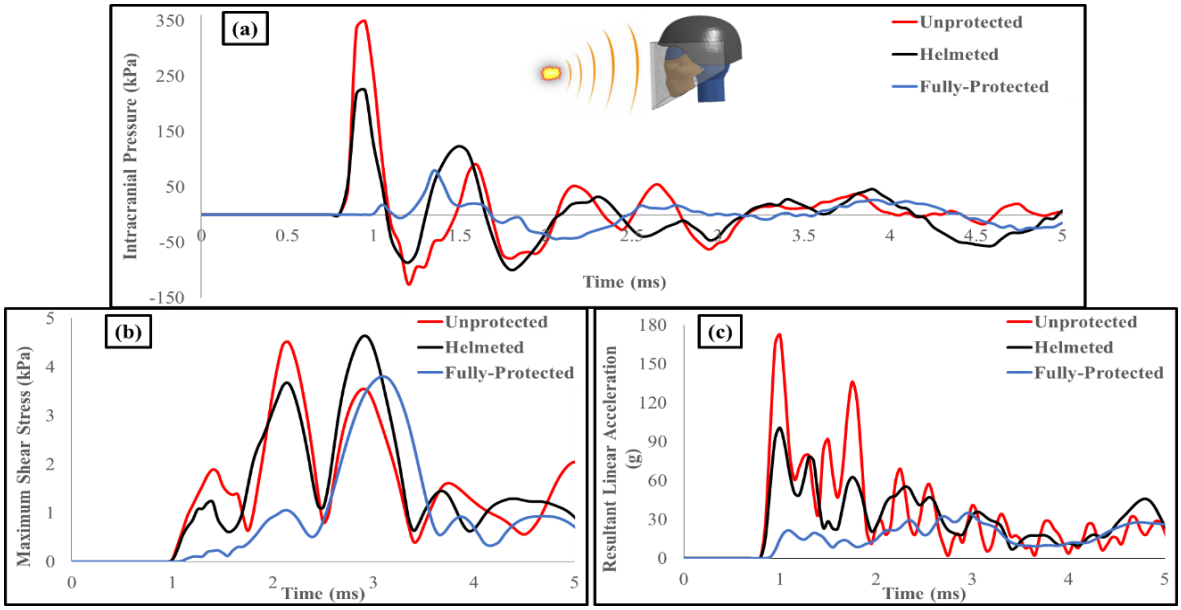

Figure 3: Time history of (a) ICP at coup site; (b) shear stress; and (c) brain acceleration for the front blast

The blast wave flow dynamics showing the propagation of the pressure waves and their interaction with the unprotected, helmeted, and fully-protected heads are shown in figure 4. These figures clearly show the impingement of the waves on the head, as well as the separation and reunion of the blast flow. Underwash effect, defined as the adverse effect of the helmet in blast conditions is manifested in the form of a localized elevated pressure region formed due to the alteration of blast flow path in the head-helmet subspace. Although the strength of this effect is highly weakened by the pads, it is still seen at the rear side of the helmeted head in the right column of figure 4(b). However, due to the diffraction of the blast waves it disappears upon using the face shield, as seen in right column of figure 4(c). The spatial variation of ICP at various intracranial locations such as cerebellum, corpus callosum, brain lobes as well as the brain stem is depicted in figure 5. The high positive (red) and negative pressure (dark blue) regions observed in the middle column of figure 5 delineate the coup and counter-coup injuries. As a possible injury mechanism, the cavitation bubbles may develop at the countercoup site of the brain due to the negative pressure field which will impose brain tissue damage upon the collapse of the bubbles. The ICP levels shown in this figure clearly magnifies the mitigation efficiency of the protection systems, i.e. helmeted and fully-protected systems.

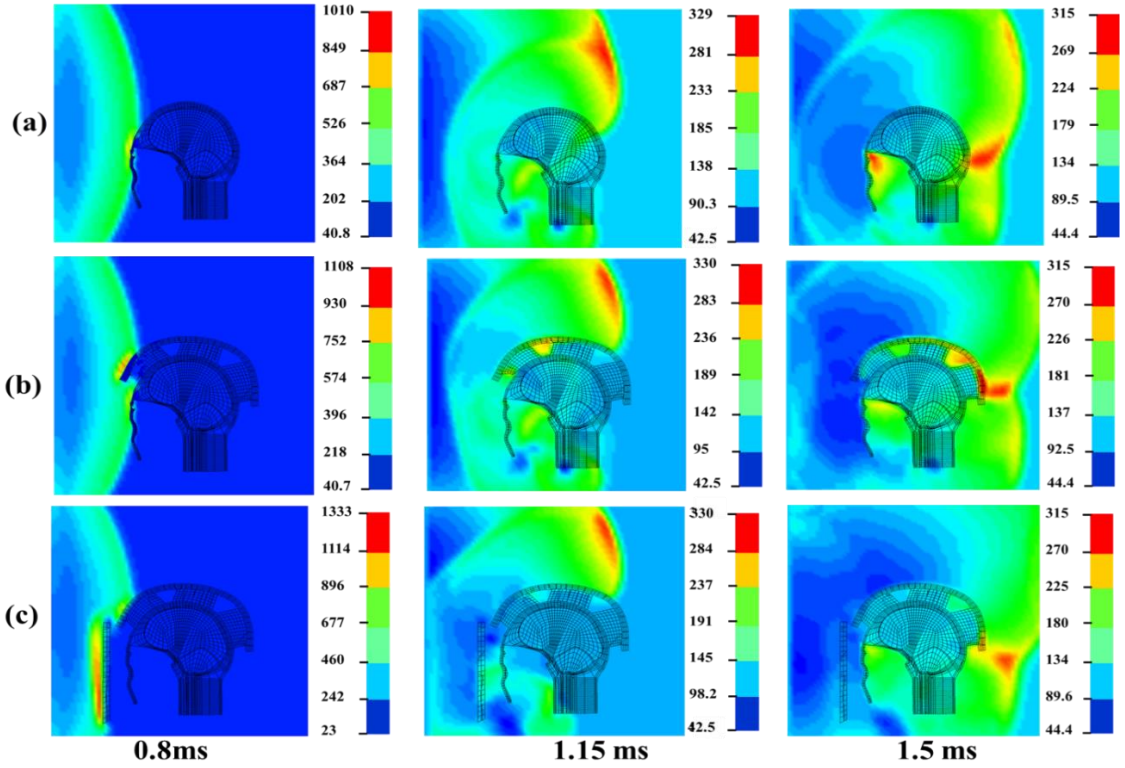

Figure 4: Blast wave propagation and interaction with (a) unprotected; (b) helmeted; and (c) fully-protected head in the front blast scenario

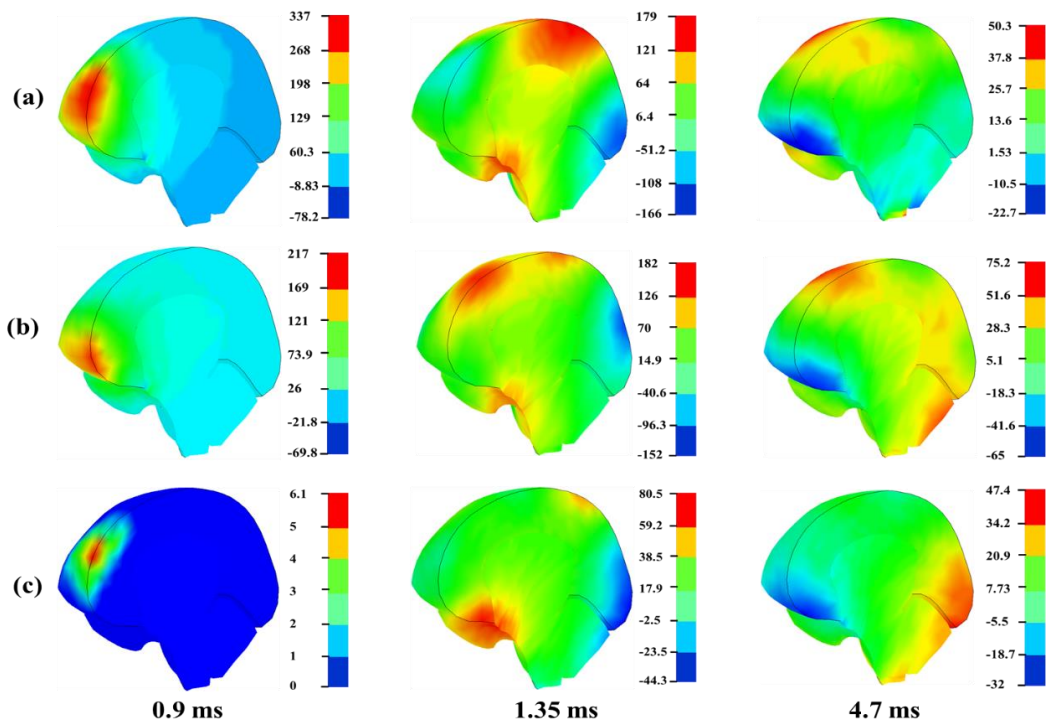

Figure 5: Spatial evolution of (a) ICP inside the brain at different time levels for (a) unprotected; (b) helmeted; and (c) fully-protected heads in the front blast scenario

3.2 Back blast scenario

The first interesting finding in studying the back blast scenario is the influence of blast directionality on the head response. As shown in figure 6(a-c), the ICP level and the acceleration of the unprotected head in the back blast is nearly twice its counterpart in the front blast scenario due to the head structural inhomogeneity, while no significant change is seen in the shear stress. As shown in figure 6(a), similar protection potentials are observed for both systems in terms of ICP levels inside the brain (about 58% reduction) as no extra protection is offered by adding the face shield in this blast scenario. In terms of the brain kinematics shown in figure 6(c), compared to 78% reduction of the acceleration upon using the helmeted assembly, the fully-protected system offers 68% (around 10% less than the helmeted case) protection. This pertains to the fact that a part of the separated blast flow approaching from the back reunites in the front and the other part is trapped inside the face shield-face gap. Hence, the sudden movement applied on the face shield upon the reflection of the entrapped turbulent shockwaves from the inner surface of the shield increases the acceleration. This condition which is clearly shown in figure 7(c) leads to the localization of the pressure waves under the face shield, hence creating an amplified pressure region in front of the face and the head. For our study, this elevated overpressure (501 kPa) corresponds to the lung injury threshold which can inflict serious facial and lung injuries as well as bTBI. Unlike the fully-protected system which elevates the overpressure around the head by 42%, the helmeted system make a 20% decrease in this overpressure. It can be clearly seen from figure 7(b) that the incidence of the underwash effect in the back blast is lower with respect to the front blast due to greater diffraction of the blast waves as well as the sharper angle of helmet curvature at the inflow of the blast waves.

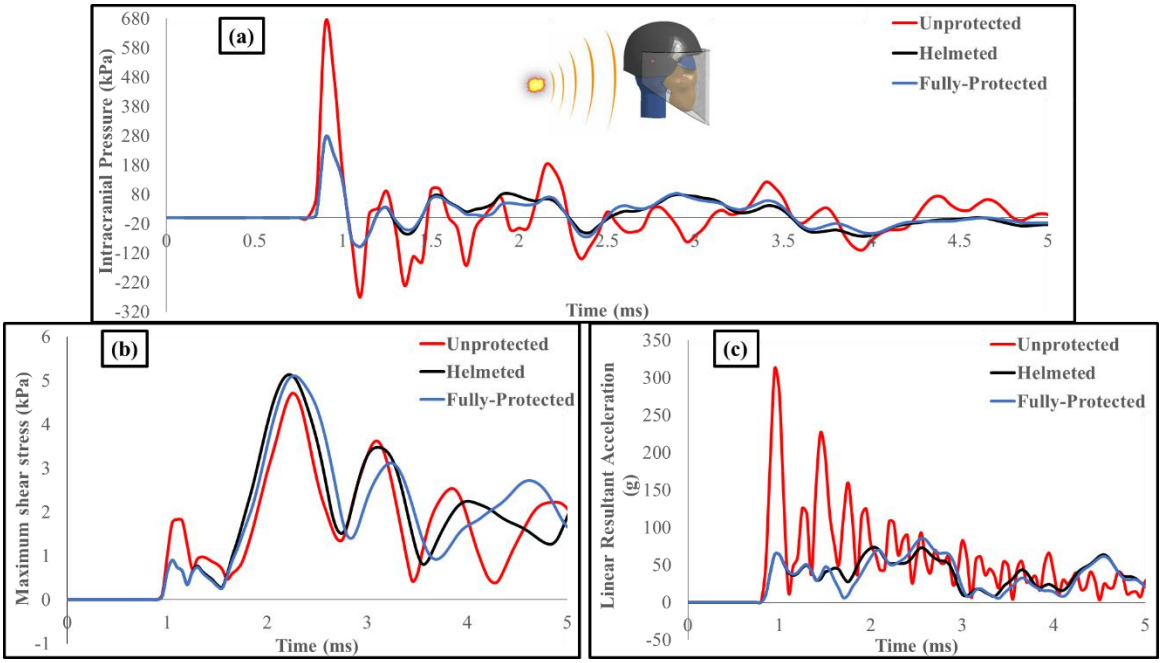

Figure 6: Time history of (a) ICP at coup site; (b) shear stress and (c) brain acceleration for the back blast

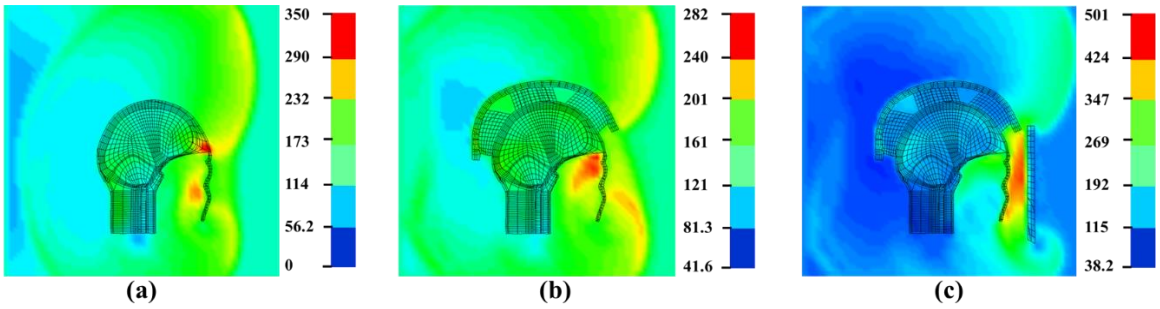

Figure 7: Reunion of propagating blast waves around the (a) unprotected head; and inside the subspace of the (b) helmeted; and (c) fully-protected heads for the back blast at t = 1.6 ms

3.3 Side blast scenario

The tissue-level response of the head as well as the brain kinematics for the side blast scenario are shown in figure 8. The directionality effect of the blast is again manifested through the alteration of brain response under the same blast overpressure due to complex geometry of the head and the protective headgears. A much greater ICP level and acceleration as well as a higher shear stress is observed for the unprotected head with respect to front and back blasts. As shown in figure 8 (a), compared to the unprotected head 67% and 87% reduction in ICP is observed for the helmeted and fully-protected cases, respectively. However, as a possible outcome of the helmet underwash effect, the helmeted assembly induces a 39% increase in the shear stress which is in contrast to the 18% reduction achieved by using the fully-protected system, as shown in figure 8 (b). The pretty high reduction of acceleration upon using the helmeted (72%) and fully-protected (83%) protection systems shown in figure 8(c) proves the effective role of the helmet and face shield in impediment of shockwaves. Similar to the back blast scenario, upon interacting with the helmet and the face shield, the incoming shock waves are diffracted and localized pressure regions are formed at the counter coup sites. Although this overpressure is smaller than the one observed for the unprotected head, but it still may bring up the concern about facial and lung injuries.

4 CONCLUSIONS

Upon studying the dynamic response of the human head under different blast loadings and using different protection levels of the head, the following were observed for the blast scenarios considered in the current study:

- It was concluded that mainly due to the structural inhomogeneity of the head and also as a result of the difference in the function and tolerance of head components, directionality of blast waves with respect to the head greatly influence the mechanical response of the head. The side blast was observed to impose the highest injury risk on the head in our study.
- It was observed that while a 77% reduction in the ICP level was observed upon using the fully-protected assembly in the front blast, 87% and only 58% reduction were observed in side and back blast scenarios, respectively confirming the highest mitigation efficacy of the protective systems in the side blast. For the front, back, and side blasts, using the helmet alone provided 37%, 58%, and 67% reduction in ICP, respectively
- Although the fully-protected model reduced the shear stress by 15% and 18% in the

front and side blasts, it increased the shear stress by 8.5% in the back blast.

- For the blast from the side and especially from the back, it was observed that the entrapment and reflection of the blast waves from the inner face of the face shield can impose serious lung and facial injuries as well as bTBI.

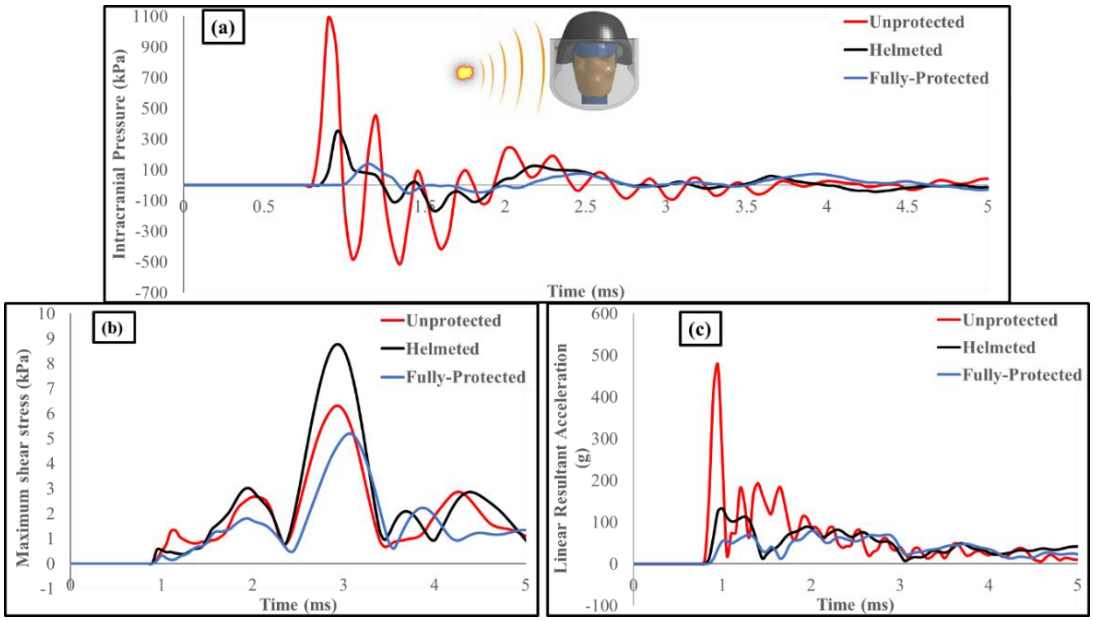

Figure 8: Time history of (a) ICP at coup site; (b) shear stress and (c) brain acceleration for the side blast;

5 REFERENCES

[1] Mathers, C. D., Lopez, A. D. and Murray, C. J. The burden of disease and mortality by condition: data, methods, and results for 2001. *Global burden of disease and risk factors* (2006) 45-88.

[2] Warden, D. L. Military TBI during the Iraq and Afghanistan wars. *J. Head Trauma Rehabil.* (2006) **21**(5): 398–402.

[3] Taber, K.H., Warden, D.L. and Hurley, R.A. Blast-related traumatic brain injury: what is known? *J. Neuropsychiatry Clin. Neurosci.* (2006) **18** (2): 141-5.

[4] Chafi, M.S., Karami, G. and Ziejewski, M. Biomechanical assessment of brain dynamic responses due to blast pressure waves. *Ann. Biomed. Eng.* (2010) **38** (2): 490-504.

[5] Ganpule, S., Alai, A., Plougonven, E. and Chandra, N. Mechanics of blast loading on the head models in the study of traumatic brain injury using experimental and computational approaches. *Biomech. Model Mechanobiol.* (2013) **12** (3): 511-531

[6] Rezaei, A., Salimi Jazi, M. and Karami, G. Computational modeling of human head under blast in confined and open spaces: primary blast injury. *Int. J. Numer. Method Biomed. Eng.* (2014) **30**(1): 69-82.

[7] Moss, W.C., King, M.J. and Blackman, E.G. Skull flexure from blast waves: a mechanism for brain injury with implications for helmet design. (2009) *Phys. Rev. Lett*. **103**:10.

[8] Grujicic, M., Bell, W.C., Pandurangan, B. and Glomski, P.S. Fluid/Structure interaction computational investigation of blast-wave mitigation efficacy of the advanced combat helmet. *J. Mater. Eng. Perform.* (2011) **20** (6): 877-893.

[9] Bowen, I., Fletcher, E.R., Richmond, D.R., Hirsch, F.G. and White, C.S. Biophysical mechanisms and scaling procedures applicable in assessing responses of the thorax energized by air-blast overpressures or by nonpenetrating missiles. *Ann. N.Y. Acad. Sci.* (1968) **152:**122–146.

[10] Horgan, T.J. and Gilchrist, M.D. Influence of FE model variability in predicting brain motion and intracranial pressure changes in head impact simulations. *Int. J. Crashworthiness* (2004) **9**(4): 401-418.

[11] Nahum, A. M., Smith, R. and Ward, C. C. Intracranial pressure dynamics during head impact. *In: Proceedings of the 21st Stapp Car Crash Conference* (2004) 337–366.

[12] Patran r2a. MSC/Patran User's Manual. MSC (2002).

[13] Altair Hyperworks. Hypermesh User's Guide, Version 11. Altair Engineering, Inc. (2011)

[14] Mendis, K., Stalnaker, R. and Advani, S. A constitutive relationship for large deformation finite element modeling of brain tissue. *J. Biomech. Eng.* (1995) **117** (3): 279.

[15] Zhang, L., Yang, K.H. and King, A.I. A proposed injury threshold for mild traumatic brain injury. *J. Biomech. Eng.* (2004) **126**: 226–236.

[16] Willinger, R. and Baumgartner, D. Numerical and physical modelling of the human head under impact-towards new injury criteria. *Int. J. Veh. Des.* (2003) **32**: 94–115

[17] Van Hoof, J., Cronin, D., Worswick, M., Williams, K. and Nandlall, D. Numerical head and composite helmet models to predict blunt trauma. *Proc. Proceedings of 19th international symposium on ballistics* (2001) 7-11.

[18] Salimi Jazi M, Rezaei, A., Karami, G., Azarmi, F. and Ziejewski, M. A computational study of influence of helmet padding materials on the human brain under ballistic impacts. *Comput. Methods Biomech. Biomed. Engin*. (2013) 1-15.

[19] Kleiven, S., von Holst, H. Consequences of head size following trauma to the human head. *J Biomech*. (2002) **35**(2):153–160

[20] Baker, W.E. *Explosions in the Air*. University of Texas Pr., (1973)

[21] Boyer, D.W. An experimental study of the explosion generated by a pressurized sphere. *J. Fluid Mech* (1960) **9**(3): 401-429.

[22] Dirisala, V. Biomechanical finite element analysis of head and neck under external loadings: a parametric study of brain response. *Dissertation*, North Dakota State University.

[23] LS-DYNA user manual, Version 971, Livermore, CA: Livermore Software Technology Corporation (2007).